Gait & Posture 29 (2009) 65–70

Contents lists available at ScienceDirect

Gait & Posture

journal homepage: www.elsevier.com/locate/gaitpost

Modeling neuromuscular effects of ankle foot orthoses (AFOs) in computer simulations of gait

Charles A. Crabtree, Jill S. Higginson *

Department of Mechanical Engineering, 126 Spencer Lab, University of Delaware, Newark, DE 19716-3140, United States

ARTICLE INFO

Article history:
Received 30 May 2007
Received in revised form 6 June 2008
Accepted 15 June 2008

Keywords:
Ankle foot orthosis
AFO
AFO model
Stroke gait
Hemiparetic gait
Muscle control
Forward dynamic simulation

ABSTRACT

Ankle foot orthoses (AFOs) provide immediate changes to gait kinematics and alter EMG-recorded muscle activity during gait; yet our understanding of neuromuscular adaptations while using AFOs remains incomplete. To address this, we have developed a tunable AFO model to predict torque from ankle angle and velocity and to identify plausible changes in muscle excitation and function in a walking simulation. Using a dynamometer in passive mode, we isolated flexion/extension torque of three polypropylene spring leaf AFOs at 5°/s, 30°/s and 120°/s, from which a model of AFO torque as a function of deformation angle, velocity and size was derived with predictive ability of $R^2 > 0.9$. The model coefficients did not vary linearly with size, illustrating the need to test AFO deformation response individually. We applied the tuned models to simulations of normal healthy gait to isolate AFO-induced neuromuscular changes. Compared to the No-AFO condition, AFO results show decreased net tibialis anterior excitation. Our results also show that net soleus excitation is not diminished with an AFO although soleus-induced ankle accelerations were reduced. With a tunable AFO model applied to walking simulations, we can quantify the contributions of muscle and orthosis to net joint torque and predict changes in neuromuscular control during walking.

1. Introduction

Properly prescribed ankle foot orthoses (AFOs) can improve gait performance and limit abnormal kinematics arising from coordination deficits [1]. Stroke patients wearing AFOs can improve gait speed [2], increase cadence and step length [3] and ipsilateral support [4]. AFOs also alter ground reaction forces in healthy adults [5]. However, neuromuscular effects are not preserved even after long-term AFO use [6]. Understanding how muscle excitation and function change in response to AFO torque can highlight abnormal muscle usage and facilitate customized motor re-training.

Three-dimensional AFO stiffness has been measured using robotic devices to prescribe ankle trajectories and detect AFO reaction moments [7]. Others outfitted AFOs with strain gauges to characterize peak stresses [8] or performed cyclic testing with a muscle training machine [9]. However, to our knowledge, neither previous study has derived a tunable AFO model from experimental data nor applied it to forward dynamic computer simulations of gait.

Forward dynamic simulations provide a platform for investigating aspects of muscle function which are difficult or impossible to measure non-invasively [10,11]. Neuromuscular control patterns have been identified via simulations [10] and provide a baseline for comparing muscle function while wearing an AFO. Although our long-term objective is to evaluate the effect of AFO usage on hemiparetic gait, simulations of pathological movements are especially challenging to develop due to issues related to muscle weakness, spasticity and other altered muscle properties [11]. Therefore, the objectives of this study were to develop a tunable AFO model and use it to investigate neuromuscular effects of wearing an AFO during normal gait. We hypothesized that AFO torque would reduce net excitation in soleus (SOL) and tibialis anterior (TA), and alter ankle accelerations induced by medial gastrocnemius (MG), SOL and TA.

2. Methods

2.1. AFO model

Three pre-molded spring leaf polypropylene AFOs (Small, Medium, Large) were selected in factory condition (i.e., no trim, strap or reshaping adjustments were made; Camp Healthcare #09400S, 09400M, 09400L). Each AFO was placed in a rubber-soled athletic shoe with a cylindrical PVC insert to stabilize the shank and minimize deformations and secured to a Biodex™ System 3 isokinetic dynamometer using heavy-duty Velcro straps (Fig. 1a). Due to shoe alignment with the

* Corresponding author. Tel.: +1 302 831 6622; fax: +1 302 831 3619.
E-mail address: higginson@udel.edu (J.S. Higginson).

0966-6362/$ – see front matter © 2008 Elsevier B.V. All rights reserved.
doi:10.1016/j.gaitpost.2008.06.004

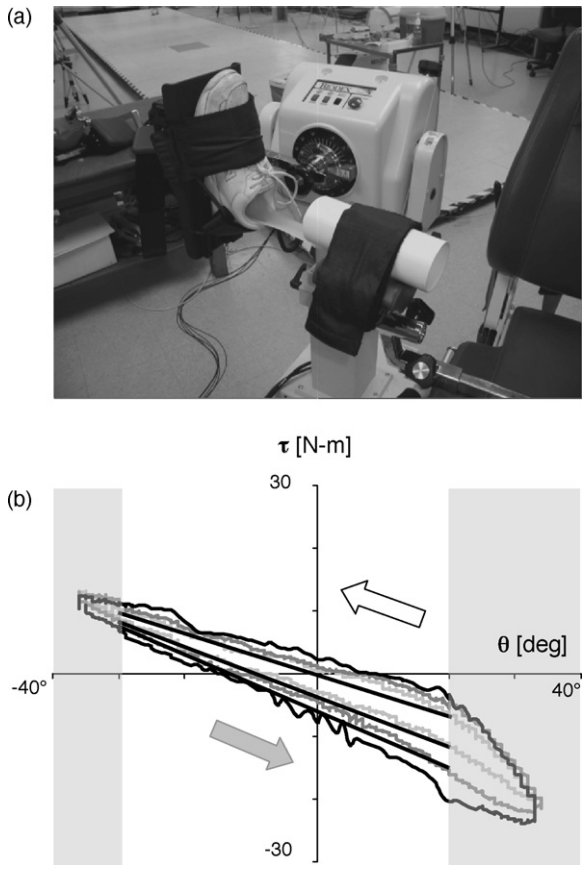

Fig. 1. Calibration of AFO torque model. (a) Each AFO was secured to a dynamometer to measure torque during passive isokinetic protocols at 5°/s, 30°/s, and 120°/s. (b) Results were post-processed to remove baseline torque and find the average torque-angle profile from five trials at each speed. Slopes (from black solid lines) and intercepts for each AFO and speed condition were fit to log and power curves, respectively. Predictive models were assembled according to a linear relation for the region of interest (unshaded) and implemented as piecewise continuous functions. Thus, separate relations were used for negative (open arrow) and positive (gray arrow) angular velocity.

dynamometer, the functional joint center was set at 7.9 ± 0.1 cm anterior and 9.0 ± 0.1 cm superior to the AFO heel and visually aligned with the rotational axis of the dynamometer in neutral position. A set of passive flexion/extension cyclic tests was defined using the dynamometer interface with "soft stops" at the end range of motion. Starting from neutral, the dynamometer sampled AFO torque, time, angular position and velocity at 1 kHz during flexion/extension at speeds of 5°/s, 30°/s and 120°/s over a range of −35° to +35° for five cycles. We also collected baseline torque due to the weight of the AFO and dynamometer attachment.

During post-processing, baseline torque was removed and averages and standard deviations were calculated over five trials per speed. Each deformation–torque plot was separated into two regions to isolate restorative torques associated with positive and negative joint velocity (Fig. 1b). The slope and intercept of each deformation–torque plot were determined at each velocity and fit to log and power curves, respectively. The power and log relations were substituted into a linear torsional spring relation resulting in a model which is a function of both joint angle and velocity:

$$\tau_{\mathrm{AFO}} = [-a \log|\dot{\theta}| - b]\theta + c|\dot{\theta}|^{d} \quad (1)$$

where coefficients a and b parameterize stiffness, c and d parameterize damping and $\dot{\theta}$ is ankle angular velocity. In a traditional torsional spring, $a = 0$, b is the spring constant, c is the damping coefficient and exponent $d = 1$; however, such a simplification was inappropriate for the material we tested (polypropylene) as it is viscoelastic.

2.2. Musculoskeletal model and simulation

A 9 DOF, 11 segment model of the musculoskeletal system was previously developed in SIMM (MusculoGraphics) using parameters representing a healthy adult male [9]. Fifteen muscles per leg were modeled as modified Hill-type actuators [12] with activation dynamics (i.e., electromechanical delay) modeled as a first-order process [13] and passive joint stiffness represented by an exponential function [14]. The AFO model was included as unilateral torque added to right ankle passive stiffness. Ground reaction forces (GRF) arise from 30 viscoelastic springs attached to a rigid foot segment [15]. Equations of motion were generated using SDFAST (PTC™).

Muscle excitations that drive the forward simulation to reproduce experimental walking patterns were optimized with a simulated annealing algorithm [16]. Errors between experimental and simulated data were minimized with a cost function composed of weighted errors of vertical and horizontal ground reaction forces, joint kinematics, joint moments and powers, and center of mass velocity. In the AFO conditions, experimental ankle moments and powers were intentionally omitted from the cost function to minimize the constraints at the ankle. Following each optimization, cost function weights were refined and further optimization performed until simulated kinematics fell within ±1 S.D. of experimental data for most of the gait cycle.

Although wearing an AFO may change the walking patterns even in unimpaired individuals, it is prescribed in order to promote normal walking patterns. Therefore, averaged kinematics and kinetics of five healthy adult men (75 kg; 180 cm) walking normally at 1.5 m/s were used for simulation and have been described previously [10,17]. Feasible muscle excitation patterns were generated for Small, Medium and Large AFO models and compared to the nominal simulation.

2.3. Analysis

Optimal muscle excitation profiles were plotted and compared between conditions. Net excitation was calculated as the area under the excitation profile for one gait cycle. Induced acceleration of each joint by selected muscles (tibialis anterior; soleus; medial gastrocnemius; vastus, VAS) was calculated directly:

$$\ddot{q}_{\mathrm{mus}} = M(q)^{-1} T_{\mathrm{mus}}(q, \dot{q}) \quad (2)$$

where $\ddot{q}_{mus}$ are muscle-induced accelerations of each generalized coordinate, $M(q)^{-1}$ is the inverse system mass matrix and $T_{\mathrm{mus}}(q, \dot{q})$ is a column vector of muscle moments with all entries set to zero except the joint(s) spanned by the muscle under consideration [18]. Kinematics and instantaneous muscle moments were exported during simulations and imported into customized MATLAB routines, thereby accounting for each muscle's instantaneous force–length–velocity characteristics. It should be noted that GRF changes due to individual muscle forces are neglected using this approach. Induced ankle accelerations due to each AFO and select muscles were compared between conditions.

3. Results

3.1. AFO model

AFO torque showed speed-dependent hysteresis, but the torque–angle relationships were nearly linear for both flexion and extension in the range of motion of normal gait. Tuned model coefficients did not scale linearly with AFO size (Table 1). The model generally achieved a predictive ability of $R^2 > 0.9$.

3.2. Musculoskeletal simulation

Simulated kinematics and GRF generally agreed with experimental data but there are notable discrepancies in moment

Table 1
AFO torque model coefficients

	a	b	c	d
AFO (L) (−)	−0.0313	−0.3672	−2.2084	0.2719
AFO (L) (+)	−0.0024	−0.3071	0.3599	0.4143
AFO (M) (−)	0.0104	−0.2420	−2.0689	−0.1117
AFO (M) (+)	−0.0122	−0.1485	0.2180	0.6583
AFO (S) (−)	−0.0095	−0.2348	−2.4086	0.0227
AFO (S) (+)	−0.0150	−0.1359	−1.193	−0.3672

Each set of coefficients/exponents corresponds to a particular AFO size and direction of restorative torque. (−) corresponds to velocities less than −5°/s and (+) to velocities greater than 5°/s. Coefficient a [N m s/rad^2] is the correction term for dynamic stiffness. Static stiffness, b [N m/rad] increases in magnitude with increasing AFO size and is larger in magnitude for negative velocity deformation. The latter is also true for linear damping coefficient, c [N m s/rad]. Exponent d [unit less] is the scaling exponent for dynamic damping correction.